Transonic Buffet Characteristics of a 60° Swept Wing with Design Variations

J. F. Mayes,* M. E. Lores,† and H. R. Barnard‡
LTV Aerospace Corporation, Dallas, Texas

Wind-tunnel tests of a typical swept wing fighter aircraft were conducted to determine the improvement in the buffet-onset lift coefficient C_{L_B}, resulting from wing camber and from leading and trailing edge deflection. The coefficient C_{L_B} was determined from trailing edge pressure, wing-root bending moment, fluorescent oil flow photographs, and force data. All four types of data are arranged in a composite graphical form to insure proper C_{L_B} selection and to identify the location on the wing where separation first occurs. Results at Mach 0.9 showed that 0.2 increase in camber (airfoil design lift coefficient) increased C_{L_B} approximately 0.08; a 5° leading edge droop 0.15; and a 5° inboard trailing edge flap 0.12. Analysis of design trends shown by previous experimental results are described for the effects of wing thickness ratio, sweep, aspect ratio, and camber on C_{L_B}. Specific buffet problems related to variable swept wings are discussed.

Nomenclature

AR	= aspect ratio
C_A	= axial force coefficient, axial force/$q_\infty S$
C_L	= lift coefficient, lift force/$q_\infty S$
C_{L_B}	= lift coefficient for initial flow separation
$C_{L_{TRIM}}$	= trimmed lift coefficient
$C_{L\alpha}$	= lift curve slope with α
C_P	= pressure coefficient, [(local) − (freestream static pressure)]/$q_\infty S$
q_∞	= freestream dynamic pressure
S	= wing reference area
t/c	= wing thickness ratio in freestream direction
$Y/(B/2)$	= fractional distance of semispan measured from wing centerline toward wing tip
α	= angle-of-attack, deg
Λ	= wing leading edge sweep back, deg
$\Lambda c/4$	= wing quarter chord sweep back, deg
σ_{rms}	= root mean square of wing bending moment fluctuation, in.-lb

I Introduction

THE evolutionary trends in combat aircraft that are currently demanding greater maneuverability in the transonic flight regime are also requiring that more consideration be given in selecting configurations that produce desirable buffet-onset characteristics. Vought Aeronautics Division (VAD) of LTV Aerospace Corporation has been conducting concentrated in-house studies to develop a better understanding of the aerodynamic phenomena causing buffet, and to identify those aircraft geometric features most tolerant of transonic flow. Of central importance in these studies are the aerodynamic disturbances that provide the driving force and the airframe structural response which ultimately establishes the cockpit environment in buffet. While the avoidance of any separated flow is not always absolutely essential for the buffet-free flight as sensed at the pilot's station, the presence of any sizable separated region provides a strong and sufficient energy source for airframe disturbance. Therefore, delaying the inception of flow separation to as high a lift coefficient as possible, particularly for transonic flight, has been the central objective of this study to select a configuration that will permit high maneuverability.

Analytical and experimental buffet investigations such as those presented by Pearcy and Holder[1] provide considerable guidance in understanding flow phenomena causing separation and buffet, and in the interpretation of trailing edge pressure divergence from wind-tunnel tests. More recently, the wing-root strain-gage wind-tunnel technique, demonstrated by Ray and Taylor,[2] permits the experimenter to obtain repeatable buffet data. The design trends established by the investigators from parametric tests will provide valuable guidance to the aerodynamicist seeking wing designs that will achieve high-buffet-free lift coefficients. Among the variables studied, wing thickness ratio, sweep, and camber were the most beneficial depending on the subsonic Mach number of interest. Application of these trends to a variable swept wing means that a wide range of the variables must be investigated to permit the inevitable trade studies to have quantitative meaning.

Very little buffet data were available at sweep angles above 40° and at higher subsonic Mach numbers. Therefore, the purpose of this paper is to provide quantitative data at higher sweep angles and at flight conditions near Mach 0.9.

II Flow Phenomena

Before presenting a detailed description of the experimental investigation, some discussion of the disturbance source and flow mechanism leading to separation is needed as a basis for properly interpreting the wind-tunnel data. Advanced aircraft with highly swept wings (particularly at wing sweeps greater than 50°) flying at transonic speeds produce extremely complex flowfields on the wing and tail surfaces. While there are four principal regions of the wing that spawn flow disturbances contributing to separation, in many cases it is the interaction of these disturbances that really cause the early depature from desirable flow conditions. Sharp leading edges certainly have their merits for some aerodynamic considerations, but they make it quite difficult to attain even modest transonic lift without contributing to significant regions of leading edge separation. If these leading edges are highly swept, the vorticity generated here and swept laterally back over the wing invariably interacts with the downstream flowfield to produce a complex flow system. The interaction of this leading edge vortex system with the viscous flowfield (particularly in the presence of vortex bursting) often contributes enough disturbance to separate the boundary layer over a large region. Characteristics near the surface caused by vortex formation are illustrated in

* Senior Engineer. Member AIAA.
† Design Engineer.
‡ Lead Engineer. Associate Member AIAA.

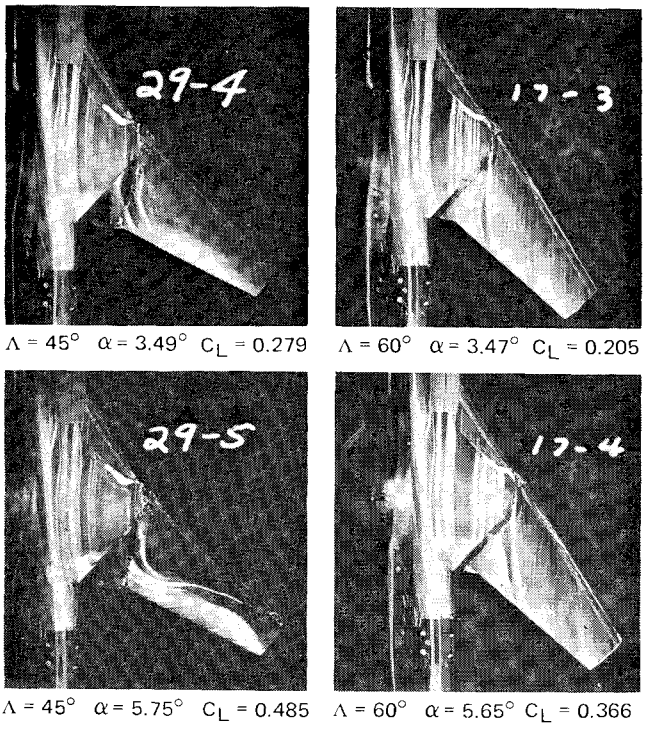

Fig. 1 Effect of wing sweep on flow pattern at Mach = 0.9.

Fig. 1 by a fluorescent oil flow photograph of a 60° swept wing at a lift coefficient of 0.366.

The wing tip sheds another vortex system and also provides the source for an undersirable shock system. Whether these factors are the source of early separation may be less important than the fact that they normally add to other disturbances and compound the likelihood of separated flow. Frequently, any shock here in transonic flow becomes part of a trailing edge shock system positioned just upstream of the wing trailing edge. Again, the area of influence can be large if the trailing edge shock is sufficiently strong to cause separation, since this frequently extends over much of the wing span. Regions of separated flow caused by shock-induced effects are illustrated in Fig. 1 for a 45° swept wing at a lift coefficient of 0.485. These regions of mixed flow and the inevitable unstable shock waves that are present in the three-dimensional wing flowfield at transonic speeds constitute the greatest hindrance to precise flow definition.

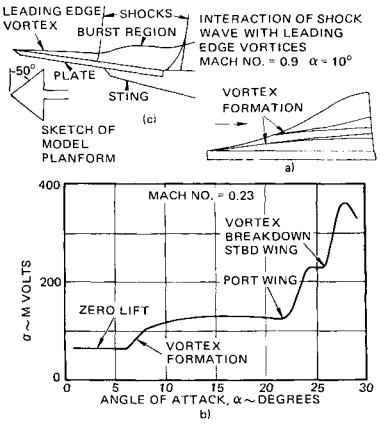

Fig. 2 Effect of vortex on strain gage data.

Sweeping the wing beyond some optimum ($\Lambda \geq 50°$) strengthens the leading edge vortex rapidly and produces a complex flowfield downstream of the leading edge that interacts with the tip system more strongly as sweep is increased. The combined effects of this vortex formation and bursting on highly swept wings at any speed, with some aspect ratio reduction effects, are strong contributions to the reduction of C_{L_B}. Vortex patterns and wing-root bending strain gage, root mean square (rms) values for a typical slender wing aircraft at low speed have been presented by Mabey.[3] As shown in Fig. 2a, the formation of one vortex system is at the leading edge of the wing-body juncture. A similar effect has been observed in flight and with water-tunnel tests of a modified F5-D aircraft as presented by Poisson-Quinton and Werle.[4] Another vortex system is generated at the slender wing of Fig. 2a midspan. Strain gage data for the model are presented in Fig. 2b to show changes in intensity for vortex formation and vortex breakdown for each wing. The same phenomena is observed at the glove-wing (fixed, inboard portion) intersection of variable sweep wings when the wing leading edge is swept less than that of the glove (see Fig. 1). In transonic flight, a trailing edge shock that may be too weak to separate the boundary layer of itself may interact with the leading edge vortex system to promote vortex bursting and initiate widespread boundary-layer separation. This bursting of the vortex by a trailing edge shock is shown in Fig. 2c as obtained from Lambourne and Bryer.[5]

It is essential that each of these individual flow characteristics be considered in developing a wing design with desirable buffet characteristics. However, analytical and intuitive methods are not sufficient to evaluate the additive or interaction effects in the flowfield. Therefore, a series of wind-

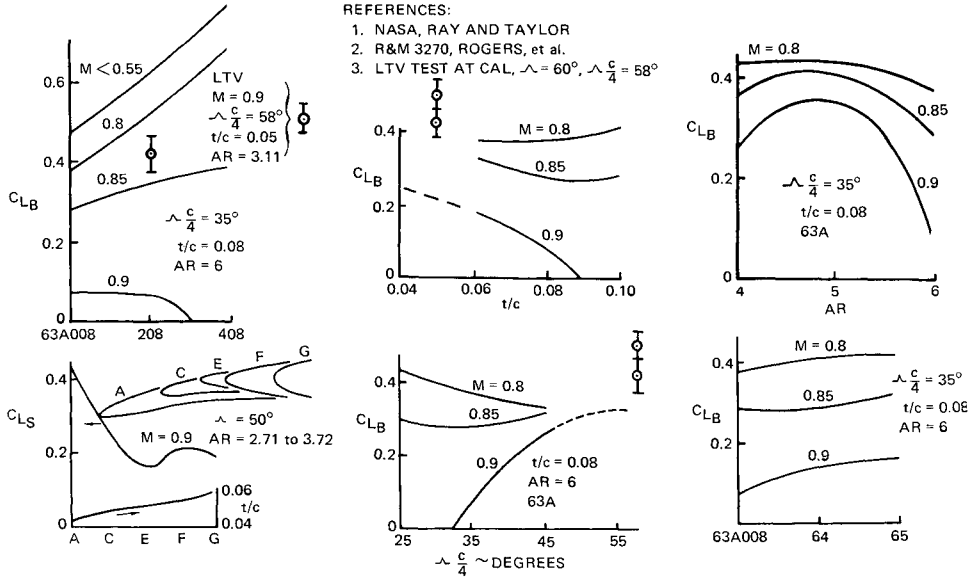

Fig. 3 Effect of wing geometry on C_{L_B}.

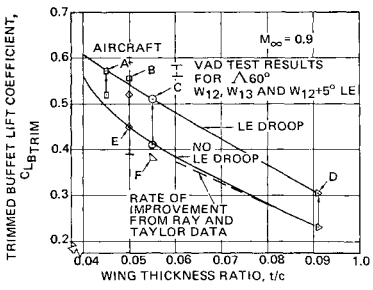

Fig. 4 Effect of wing thickness ratio on buffet lift coefficient.

tunnel buffet tests were conducted to provide direction for development of improved wing configurations. Several types of data were obtained in these tests to give basis for meaningful interpretation of the flow phenomena, particularly at the critical high-subsonic flight conditions.

III Selection of Test Configuration

A study of available parametric buffet data, with an understanding of the flow phenomena, was necessary before selecting wing geometry combinations with the greatest potential for high-buffet-free performance. Recent buffet tests conducted in the NASA Langley Field wind tunnel by Ray and Taylor[2] show the effect of wing sweep (Λ), thickness ratio (t/c), aspect ratio (AR), position of maximum thickness, and camber. Values of C_{L_B} were obtained by interpreting the divergence of α rms vs C_L, presented by Ray and Taylor,[2] and plotting these results as shown in Fig. 3. Of particular importance is the variation of C_{L_B} with camber. The basic wing with a $\Lambda c/4$ of 35°, t/c of 0.08, AR of 6.0, and no camber is shown with test values for 0.2 and 0.4 camber wings with the other variables held constant. Lines of constant free-stream Mach number (0.55, 0.8, 0.85, and 0.9) are plotted to show the effect of Mach number as camber is increased. The reduction of C_{L_B} at Mach 0.9 is believed to be caused by the effective thickening of the airfoil caused by camber. Movement of the approximate maximum t/c position from 30–50% provides some improvement of C_{L_B} as might be expected. The effect of wing t/c on C_{L_B} is shown for the basic configuration and for wings with $t/c = 0.06$ and 0.10. A decrease of about 0.1 in C_{L_B} is obtained by increasing the thickness ratio from 0.06–0.08 at Mach 0.9. This same strong trend will be shown later by flight test data. Of possibly greater importance is the reduction of C_{L_B} with aspect ratio. A decrease of better than 0.25 in C_{L_B} or 78% is obtained by increasing the aspect ratio from 5 to 6 at Mach 0.9. The shape of these curves indicate an optimum aspect ratio exists near 5.0, and the trend is most predominant at Mach 0.9. The 0.1 increase in C_{L_B}, obtained by increasing the aspect ratio from 4 to 5, is understandable; i.e., C_L should increase in porportion to AR. The decrease in C_{L_B} for an AR of 6.0 is more difficult to understand. A possible explanation is the intersection of a forward shock and rear shock in the tip region, forming a single strong outboard shock with its attendant separation. It is possible that such an intersection is avoided for the lower AR wing. Discussions of these flow phenomena are presented by E. W. E. Rogers et al.[6] The value of C_{L_B} for the AR of 6.0 wing at Mach 0.9 is significantly improved by increasing the sweep at the quarter chord to 45°. The comparatively flat variations of C_{L_B} with sweep for Mach 0.85 and 0.8 suggest that the Mach number normal to the leading edge or wing isobars are of greatest importance in understanding the sweep effect. Achieving local subcritical flow and reducing the possibility of shock-induced separation is a vital factor in obtaining high-buffet-free design. To this end, inviscid three-dimensional theoretical calculations can be instructive in determining the wing shape.

The improvement in lift coefficient for incipient separation C_{L_S} obtained by reducing thickness ratio, and increasing leading edge camber are shown in Fig. 3.[6] Both leading and trailing edge sweep angles of this wing are 50°. The geometry modifications from G to A were obtained by increasing the chord length which in turn reduces the aspect ratio from 3.72 to 2.71 and reduces the thickness ratio from 5.97 to 4.36%. Greatest improvement in C_{L_S} is achieved by increasing the leading edge camber.

Flight test results at Mach 0.9 also show the improvement of leading edge camber as simulated by leading edge droop. Trimmed lift coefficients for buffet onset of operational aircraft provided by Lindsay[7] at Mach 0.9 are plotted vs the average wing thickness ratio presented in Fig. 4. Lines are faired through data for aircraft with leading edge droop and without leading edge droop. A very strong trend is shown for buffet improvement with decrease in thickness ratio. Leading edge droop provides an incremental improvement in C_{L_B} of 0.05–0.10. The rate of improvement obtained by the Ray and Taylor data in Fig. 3 has been superimposed to show agreement when t/c is reduced from 0.08 to 0.06. The actual magnitude of C_{L_B} should not be the same since the data of Fig. 3 are for an aspect ratio 6 wing which is significantly higher than for the aircraft cited in Fig. 4. If the increment of 0.25 obtained by reducing AR from 6 to 5 is added to the C_{L_B} from Fig. 3, then the magnitudes agree more closely with the flight test data of Fig. 4.

With these data and observations in mind, some general statements can be made for the design of lifting surfaces to achieve high-buffet-free lift at or near a flight Mach number of 0.9: 1) Wing thickness ratio should be as low as structural limitations will permit; 2) Increased wing sweep will permit higher thickness ratios to be used; 3) Camber or leading edge droop can be used provided sufficient wing sweep is also used; 4) For any combination of the aforementioned variables, an optimum aspect ratio may exist; and 5) Wing-root design and wing-body fairing is important and highly configuration-dependent. Rapid increase in body cross section near the wing trailing edge, shown in Fig. 1, obviously contributed to local separation in that region.

The previously mentioned statements provide some qualitative guidance to the aerodynamicist, but do not show how to achieve the optimum combination of variables and the quantitative results to be expected. An experimental program was formulated to investigate the quantitative benefits that might be derived from a judicious application of the aforementioned trends, and to provide data for future development of prediction methods which would permit selection of the best combination of wing geometric variables.

A wing with a leading edge sweep of 60° and thickness ratio of 0.05 was selected to permit increase of camber from 0.2–0.4 without encountering severe shock-induced effects. (A camber of 0.2 as expressed here means a two-dimension streamwise section with a design lift coefficient of 0.2.) Simulation of camber, often necessary for practical design, was obtained by a 5° leading edge droop and a 5° trailing edge flap. No attempt was made to optimize this angle. Only basic design trends and magnitudes were desired.

IV Wind-Tunnel Model Instrumentation and Data Reduction

Theoretical studies of lifting surface aerodynamics are useful to show some trends, but the inability to accurately deal with the viscous flowfield in a mathematical analysis has continued to require numerous wind-tunnel tests of the configuration variables. Even the wind tunnel does not yet provide any one source of data that can be interpreted as to full-scale separation characteristics without some uncertainty. The most dependable buffet testing method found is that of Ray and Taylor.[2] Simultaneous acquisition of wing-root bending moment fluctuations, trailing edge pressure over the complete span, six-component force data, and oil flow are all important in predicting buffet onset. This approach also permitted location of regions on the wings

or tail where boundary-layer separation occurs. All four types of data are used to establish the angle-of-attack and lift coefficient for buffet onset. This approach is mandatory for highly swept wings where there is considerable difficulty in interpretation of wing or tail strain gage data. In the case of variable swept wings with strain gage located outboard of the pivot, it is questionable whether the gage will respond to separated regions inboard. Also, the gradual increase in rms level with angle-of-attack without a sharp rise of intensity makes the investigator more dependent on trailing edge pressure and oil flow data to establish the region of onset C_L

Model Description

Results of VAD variable sweep wing tests at Cornell (see Fig. 1), as well as the parametric tests of Ray and Taylor (see Fig. 3), pointed to the importance of proper wing thickness ratio and camber as best solutions to the buffet problem at high subsonic Mach numbers. A limited test program using three wings with a sweep of 60° was conducted to provide a basis for understanding the relative importance and benefits of thickness ratio and camber. Significant features of each wing are listed in Table 1.

As shown in Fig. 5, W_{12} has a constant 0.2 camber and provisions for leading and trailing edge droop. W_{13} has a constant 0.4 camber with mean line a equal to 0.5 as does W_{12}. W_{14} is an isobar design using the recommendations of Lock.[8,9] Effects of camber were determined from W_{12} and W_{13}. Leading and trailing edge droop on W_{12} permitted evaluation of these devices in producing increased camber. W_{14} provided information as to the effect of camber variation with span and leading edge tip shape. Inboard and outboard glove designs representative of full-scale thickness and contour were fabricated and tested on each wing.

Instrumentation and Data Reduction

This test was conducted in the 8-ft, continuous-flow, transonic wind tunnel at Cornell Aeronautical Laboratory under the conditions shown in Fig. 8.

Basic force and moment data for this study were acquired by using a six-component internal strain gage balance employing standard data reduction techniques to reduce the data to coefficient form.

To obtain data consistent with that presented by Ray and Taylor,[2] the transition strip was located in accordance with the recommendations of Braslow, et al.[10] The transition strip was consistently located 0.5-in. aft of the wing leading edge and was 0.1-in. wide. The strip was made using Number 220 carborundum grit and care was taken to insure that the grit was not too dense.

To obtain discernible buffet-onset points, three additional types of data were obtained, namely rms bending moment fluctuations at the wing-root, wing trailing edge pressure divergence, and fluorescent oil flow studies of the upper and lower wing surface. These three techniques are discussed below.

Obtaining buffet-onset points from the rms bending moment fluctuations provides additional problems not normally experienced in force and pressure tests: 1) The high temperatures associated with a continuous flow wind tunnel precludes the use of semiconductor strain gages. To avoid this problem, foil gages (BLH 120 Ω) were mounted on the upper and lower surface of the wing; 2) Placement of the strain gage on the wing is critical because of the desirability to have maximum strain occur at the strain gage location for a given fluctuation of the wing loading; and 3) Specific time intervals are required at each data point for the rms equipment to function properly. This time interval may vary considerably between wind tunnels depending upon several factors including tunnel turbulence, model support system, etc. Ray and Taylor[2] have indicated time intervals on the order of 45 sec are necessary for repeatable rms buffet data. Ray and Taylor's rms buffet data were integrated and averaged over the 45-sec time interval to give an average rms bending moment.

Table 1 Significant wing features

Wing	Airfoil section	W_{12}, W_{13}, W_{14}
W_{12}	65A205 a = 0.5	AR (Λ = 60°) = 3.11 Taper ratio = 0.33 Span, in. = 22.00
W_{13}	65A405 a = 0.5	
W_{14}	63A006 at $Y/(B/2)$ = 0.227; 65A205 a = 1 at $Y/(B/2)$ = 0.846	

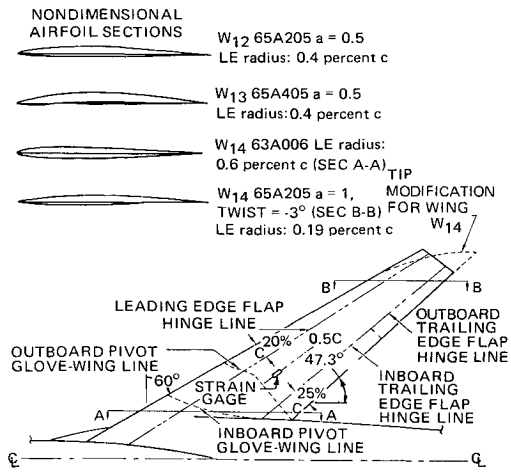

Fig. 5 Wind-tunnel model geometry.

The data presented in this paper were not averaged but were based on an instantaneous value from the rms meter. Simplified schematic diagrams of the two types of circuits are shown with the Langley circuit in Fig. 6 to illustrate methods of integration to obtain σ rms. A direct comparison of the instantaneous method and time average methods was obtained in the Cornell wind tunnel and the data for two typical cases are presented in Fig. 7. As can be seen, the two methods compare favorably as far as selecting the lift coefficient at buffet onset. The importance of careful integration averaging of the σ rms signal is believed to be primarily a function of the stability of drift in tunnel flow conditions.

Complementing the wing-root bending moment fluctuation method is the wing trailing edge pressure divergence method. Eight-static pressure orifices were located on both the upper and lower wing panel. These orifices were located three in. from the model centerline to ten in. from the model centerline with 1-in. increments. Each orifice was located at 95% of the local streamwise chord. Pressure lines were routed to the base of the sting support system where a scanivalve was located. The scanivalve had a sampling rate of

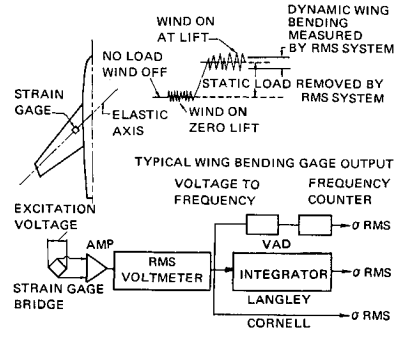

Fig. 6 Wing strain gage instrumentation.

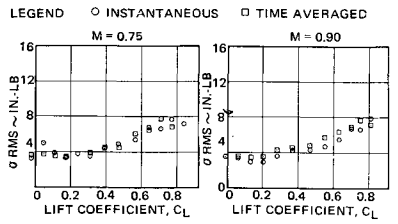

Fig. 7 Comparison of time averaged with instantaneous σ_{rms}.

approximately one orifice. The pressure data were reduced to standard coefficient form for analysis.

An extensive fluorescent oil flow study was conducted on the upper and lower surface of the right-hand wing so as not to interfere with the pressure orifices located on the left-hand wing. Cameras were located in the ceiling and floor of the test section to obtain simultaneous photographs of the upper and lower wing surface at each selected angle-of-attack.

V Wind-Tunnel Test Results

Both experimental and theoretical studies of the wings described above were performed to provide adequate understanding of the qualitative and quantitative effects of buffet. Wind-tunnel tests at Cornell provided force, strain gage, trailing edge pressure, and fluorescent oil flow data. A composite presentation of these data is shown in Fig. 8 for W_{12} at Mach 0.9. Trailing edge pressure for other Mach numbers are shown since evaluation of the divergence with Mach number, as well as angle-of-attack, is important.[1] Oil flow photographs are presented for angles-of-attack before and into separation. Interpreting these data for the purpose of identifying aerodynamic disturbances that will be related to buffet onset was accomplished by: 1) identifying the last data point of low-intensity (usually tunnel turbulence[2]) strain gage data and the next data point in the transition to the first plateau; 2) angle-of-attack lines are drawn from these points to the C_L vs α curve to identify the band of lift coefficients for transition; 3) the lines are extended through the trailing edge pressure variations to determine which region of the wing is separated first and to verify that the strain gage is sensing inboard separation if it exists; 4) angle-of-attack lines are also extended to the axial force variation to provide added assurance of the onset values. Here the reflex of the curve is used to indicate the departure from leading edge suction as suggested by Ray and Taylor[2] and Rogers, et al.[6]; and 5) the oil flow photographs are studied to identify the effects at or near the span station where pressure coefficient divergence exists and to determine the cause of these effects.

Using the previous guidelines, W_{12} (see Fig. 8) shows a C_{L_B} to exist between 0.38 and 0.46 (angle-of-attack of 4.8° and 5.9°) for 0.9 Mach number, Since the purpose of these tests was to establish relative benefits of the selected configurations, no effort was made to obtain additional strain gage data within the C_{L_B} range previously stated or by other means to establish a finite value of C_{L_B}. It was considered important in this investigation to avoid either a conservative or optimistic interpretation of the data. At Mach 0.9, the trailing edge pressure (C_P) variation with angle-of-attack is well behaved; i.e., remains essentially constant. A slight divergence is noted at orifices 2, 6, and 7. The slight rate of C_P negative increase with angle-of-attack corresponds, as expected, with that of σ rms between an angle-of-attack of 4.8° and 5.9°. Very little divergence of C_P with Mach number at constant angle-of-attack is observed below 5.9°. To examine this divergence more closely, a cross plot of the Mach 0.75, 0.85, 0.9, and 0.92 C_P vs angle-of-attack curves at constant angle-of-attack would be necessary. Theoretical values of leading edge suction as recommended by Ray and Taylor[2] were not computed. It has been observed that near Mach 0.9 this divergence of the theoretical value from the experimental, indicating buffet onset, normally occurs near the reflex of the C_A vs the angle-of-attack curve.[6] The reflex does appear for the C_A curve at approximately 4.8°.

Fluorescent oil flow photographs are shown in Fig. 8 for an angle-of-attack of 3.67°, 6.00,° and 8.33°. A slight breakdown in the leading edge system is observed at 6°. Further deterioration of this system is shown at an angle-of-attack of 8.33°, and the reversal of the boundary layer in the tip trailing edge region shows definite separation. This is confirmed by the large C_P divergence at tap 2 for values of an angle-of-attack above 6°. The range of C_{L_B} for W_{12} and W_{13} is superimposed on the parametric data shown in Fig. 3. The level of C_{L_B} achieved approaches that obtained for the 35° swept wing at Mach 0.8. Therefore, the benefit of sweep in permitting the use of camber is demonstrated. From these results, it is apparent that redesign of the wing tip would be beneficial.

A slight twist or washout to reduce the higher effective angle-of-attack and some reduction of thickness ratio would be helpful in the tip region.

It is important at this point to observe that no single type of data provides the necessary guidance for selecting the lift coefficient of buffet onset and the region of the wing where significant separation occurs. The four types of data used here are believed to be necessary for adequate buffet analysis. Presentation of all four types of data in a composite form on the same sheet provides an efficient means of properly interpreting the test results. In many cases, the cause of separation and possible remedies can be more easily determined from the data in this format.

A composite of test results for W_{13} is presented in Fig. 9. A slightly lower range of angle-of-attack 4.7° and 5.9° is indicated by the strain gage rms values than obtained for W_{12}. The C_{L_B} values, 0.46 to 0.535, are higher because of the increase in camber from 0.2 to 0.4. The trailing edge pressure divergence is small but discernible from tap 2 inboard at values of slightly below 4.3°. The oil flow photograph at an angle-of-attack of 3.57° shows slight separation near the trailing edge in the tip region and near the wing-body juncture. The divergence of trailing edge pressure with Mach number for the inboard region confirms the existence

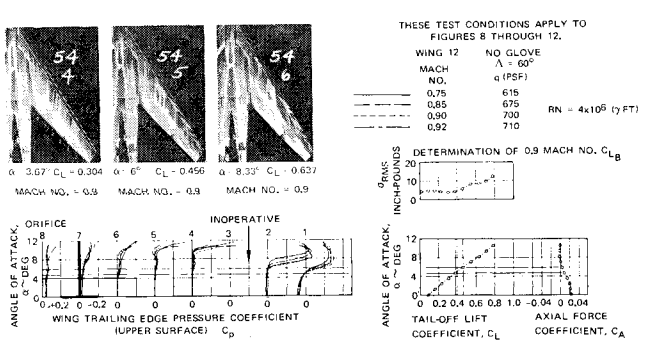

Fig. 8 Wing 12, composite of wind-tunnel data.

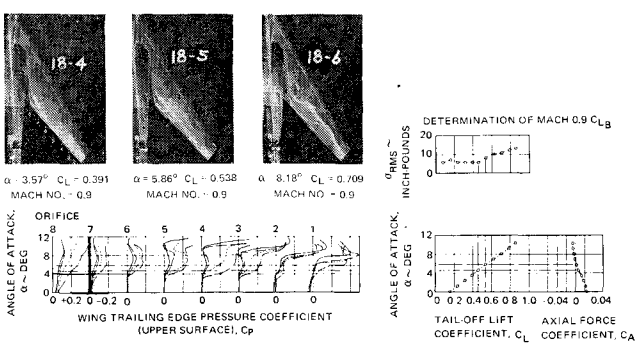

Fig. 9 Wing 13, composite of wind-tunnel data.

of separation at lower values of angle-of-attack. Strain gage fluctuations do not show this effect due to location of the gage (see Fig. 5). Inboard separation is too near the gage, and tip separation affects only a small area. At angles-of-attack above 5° (see oil flow at an angle-of-attack of 5.86°), shock-induced separation inboard is significant and diminishes toward the tip. A decrease of the body cross-sectional area or waisting, as suggested by Rogers, et al.,[6] would undoubtedly decrease the inboard shock strength and the attendant separation. At these angles-of-attack, trailing edge pressure divergence appears over the entire span. The divergence of trailing edge pressure for a Mach number of 0.92 suggests that further increase in camber would not be beneficial at 0.9, since the appearance of shock-induced separation is occurring at such low-angles-of-attack. The effective increase in thickness ratio and trailing edge slope resulting from increased camber would aggravate the separation observed for the 0.4 camber wing. Buffet lift coefficients obtained for W_{12} and W_{13} are presented in Fig. 3 to show the relative improvement of a cambered swept wing over that for wings of lower sweep and higher thickness ratio. The results are also shown in Fig. 4 to illustrate compatibility with flight results for aircraft with a t/c of 5%.

The test results for the W_{14} isobar wing are presented in Fig. 10. A slight transition region for C_{L_B} of 0.25 to 0.325 is indicated by the strain gage data; however, no divergence of trailing edge pressure or significant separation region is indicated in the oil flow photographs at C_L values below 0.325. Therefore, the next highest test point 0.325 was chosen for the lower value of C_{L_B} transition and 0.42 for the higher value. Trailing edge pressure divergence is well established at a C_L of 0.42 which corresponds to an angle-of-attack of 4.7°. The oil flow photograph for an angle-of-attack of 5.83° shows separation near the trailing edge and outboard from orifice 4. Trailing edge pressure divergence confirms the separation. The shape of the axial force variation indicates a lower transition region for C_{L_B}.

Results for W_{14} were disappointing; however, valuable information was derived from the test data. The increased slope at the trailing edge defined by a mean line a equal to 1.0 for the tip section, and the gradual change in geometry to a symmetrical 63A006 airfoil near the root, obviously caused early low-angle-of-attack separation over about 40% of the exposed outboard region. Although W_{14} had twist to reduce the effective angle-of-attack at the tip, it appears that the trailing edge slope was more critical.

The most impressive results obtained for this series of tests are shown in Fig. 11 for W_{12} with 5° leading edge droop. Strain gage rms data show a C_{L_B} transition between 0.525 and 0.61. The unusually high rms value of 17.5 at C_L of 0.61 and the decreasing trend as angle-of-attack is increased was not observed for the other configurations. Repeat runs obtained during oil flow tests provided confirmation of the trend. A possible explanation is that some degree of coupling between the structural characteristics of the aluminum wing and aerodynamic load fluctuations occurred for C_L values above 0.525.

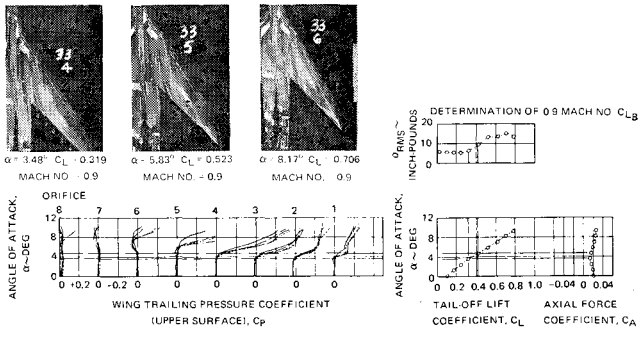

Fig. 10 Wing 14, composite of wind-tunnel data.

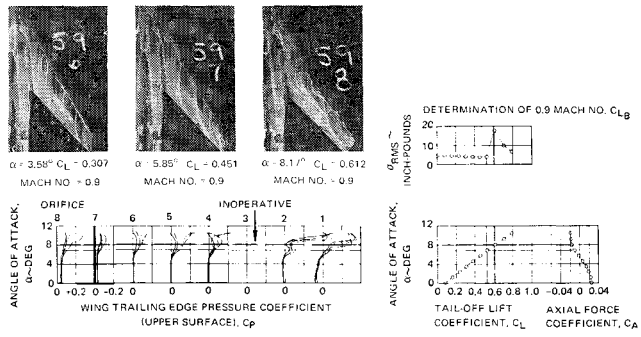

Fig. 11 Wing 12, 5° leading edge droop, composite of wind-tunnel data.

Only slight divergence of the trailing edge pressure with angle-of-attack or Mach number is shown for angles-of-attack below 5.9°. The intercept of this angle with the C_A variation appears reasonably close to the reflex of the curve. Well behaved flow is shown in the oil flow photograph for an angle-of-attack equal to 5.85° both at the leading and trailing edge.

Results of the leading edge droop tests suggest that leading edge camber is more effective in achieving high values of C_{L_B} than camber of the entire chord or mean line. As with W_{13} and W_{14}, this suggests the importance of the slope at the trailing edge being as small as possible. Further evidence of this trend is shown by the lower C_{L_B} values obtained for W_{12} with 5° leading and trailing edge flap deflection (see Fig. 12). Deflection of the outboard flap reduces C_{L_B} even further as shown by the results presented in Fig. 12.

Both inboard and outboard glove configurations shown in Fig. 5 were tested on each of the three wings. The purpose of these tests was to determine the effect on C_{L_B} of increased thickness ratio and surface slope discontinuities at the wing-glove intersection. The glove modifications did not reduce the value of C_{L_B} for W_{12} or W_{14}, which indicated that the inboard regions of these wings were not critical with regard to thickness ratio. A surprising result was the slight increase in C_{L_B} obtained for W_{13} with both glove configurations. The improvement indicated is within the uncertainty of the onset transition and is not considered significant. The fact that the glove additions to all three wings did not cause reduction in C_{L_B} is considered significant.

VI Theoretical Chordwise Pressure Distributions

Wind-tunnel tests of these wings provided gross insight to the flowfield characteristics. However, more detailed local flow information, particularly the pressure gradients and boundary-layer development, is valuable in assessing the susceptibility of the flow to separation. Therefore, theoretical chord-wise pressure coefficients were computed for W_{12}, W_{13}, and W_{14} to compare the predicted flow characteristics for these various configurations. Although three-dimensional transonic flowfield calculations, including shock, boundary-layer interaction, are beyond the state-of-the-art,

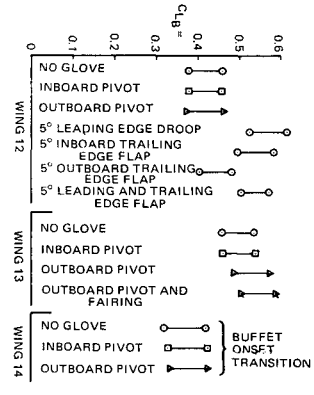

Fig. 12 Summary of buffet wind-tunnel data for wings 12, 13, and 14 at Mach 0.9.

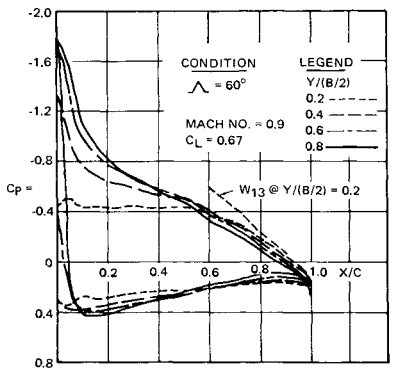

Fig. 13 Wing 12 theoretical chord wise pressure distributions.

inviscid, subcritical flow with a compressibility correction are helpful in the design analysis. A digital computer program, based on the methods derived from Kuchemann[11] and Brebner[12,13] was used to compute chordwise pressure distributions for span stations of 0.2, 0.4, 0.6, and 0.8 $Y/(B/2)$. The computer program provides predictions of pressure distributions for wings of finite thickness and arbitrary planform in attached, inviscid, subcritical flow. A leading edge correction factor which is a function of the leading edge sweep angle is included in the program.

Figure 13 shows typical results for W_{12} with outboard glove. The importance of bringing the leading edge more in line with the upwash for the outboard region is shown by the undesirably high-negative pressure coefficients obtained in that region. These low pressures are part of the mechanism that produces the pressure gradients and velocity patterns causing local separation and leading edge vortex system for highly swept wings. Additional leading edge radius or camber provide a surface more easily followed by the streamline; i.e., reducing the initial sharp expansion region reduces the separation region.

Pressure gradients approaching the trailing edge are critical for the inboard stations where glove thickness ratio becomes important. The computed pressure distributions near the trailing edge of W_{13} at 0.2 span station is shown to illustrate the increased gradient contributing to the inboard separation observed in the test results.

VII Conclusions and Recommendations

The following conclusions are given within the scope of geometry and test conditions of this paper. It is believed that the design trends are applicable to wings with 50°–65° of sweep and airfoil sections with approximately the same streamwise thickness ratio and maximum thickness position. The conclusions are: 1) Wind-tunnel results confirmed the validity of using the Mach number normal to the leading edge to relate the buffet improvement trend for wings with low sweep to that of wings with high sweep for the same streamwise camber; 2) Leading or trailing edge droop provides about the same buffet improvement as increasing camber from 0.2–0.4. Simultaneous use of leading and trailing edge droop does not improve buffet characteristics over that for each device used separately; 3) Use of an airfoil with a mean line definition of $a = 1.0$ increases the upper surface edge slope and produces early separation; 4) Buffet lift coefficients obtained in the VAD tests are compatible with previous wind-tunnel and flight test results (see Figs. 3 and 4); and 5) Presentation of wind-tunnel buffet data in composite form enables the investigator to identify buffet-onset lift coefficient and the region on the wing where separation occurs. In many cases the cause of separation and possible remedies can be more easily determined from the data in this format.

Although the testing techniques, analysis, and wing design information presented in this paper are important contributions to preliminary aircraft design, additional techniques and methods of analysis are necessary for predicting buffet onset for full-scale aircraft when onset is defined by a given magnitude of vibration at the pilot station or at the center of gravity. In the writers' opinion, wind-tunnel instrumentation should include pressure transducers to provide load fluctuation and frequency data. An analysis using the just mentioned forcing function, properly scaled, with proper representation of structural response may provide the required intensity prediction at selected body stations.

References

[1] Pearcy, H. H. and Holder, D. W., "Simple Methods for the Prediction of Wing Buffeting Resulting from Bubble-Type Separation," NPL Aero Rept. 1024, July 1962, National Physical Laboratory.

[2] Ray, E. J. and Taylor, R. T., "Buffet and Static Aerodynamics Characteristics of a Systematic Series of Wings Determined from a Subsonic Wind-Tunnel Study," IND-5805, June 1970, NASA.

[3] Mabey, D. G., "Measurements of Buffeting on Slender Wing Models," C.P. 917, 1967, Aeronautical Research Center.

[4] Poisson-Quinton, P. and Werle, H., "Water Tunnel Visualization of Vortex Flow," *Astronautics and Aeronautics*, Vol. 5, No. 6, June 1967, pp. 64–66.

[5] Lambourne, N. C. and Bryer, D. W., "The Bursting of Leading-Edge Vortices—Some Observations and Discussion of the Phenomenon," R&M 3282, 1962 Aeronautical Research Center.

[6] Rogers, E. W. E., Berry, C. J., and Townsend, J. "A Study of the Effect of Leading-Edge Modifications on the Flow over a 50-deg Sweptback Wing at Transonic Speeds," R&M No. 3270, May 1960 Aeronautical Research Center.

[7] Lindsay, T. L., "A Procedure for Estimating Buffet Onset Normal Force as Effected by Wing Geometry," TN AL-70, June 1968, Naval Ships Research and Development Center.

[8] Lock, R. C., "The Design of Wing Planforms for Transonic Speeds," *Aero Quarterly*, Vol. 12, Feb. 1961, p. 65.

[9] Lock, R. C. and Rogers, E. W. E., "Aerodynamic Design of Swept Wings and Bodies for Transonic Speeds," *Advances in Aero Sciences*, Vol. 3, 1961, pp. 253–275.

[10] Braslow, A. L. et al., "Use of Grit-Type Boundary Layer Transition Trips on Wind-Tunnel Models," TN D-3579, 1966, NASA.

[11] Kuchemann, D., "A Simple Method for Calculating the Span and Chordwise Loading on Straight and Swept Wings of any Given Aspect Ratio at Subsonic Speeds," R&M No. 2935, Aug. 1952 Aeronautical Research Center.

[12] Brebner, G. G., "The Calculation of the Loading and Pressure Distribution on Cranked Wings," R&M No. 2947, Jan. 1953 Aeronautical Research Center.

[13] Brebner, G. G., "The Application of Camber and Twist to Swept Wings in Incompressible Flow," Rept. Aero 2458, March 1952, Royal Aircraft Establishment.